Reprinted from February 1979, Vol. 101, Journal of Pressure Vessel Technology

An Analysis of a Wire-Wrapped Mechanical Crack Arrester for Pressurized Pipelines

L. B. FREUND

V. C. F. LI

Division of Engineering,
Brown University,
Providence, R.I. 02912

D. M. PARKS

Department of Engineering
and Applied Science,
Yale University,
New Haven, Conn. 06520

Because of the difficulties which have been encountered in efforts to establish fracture toughness standards for arrest of running shear fractures in pressurized pipelines, the possibility of introducing mechanical crack arresters on such pipelines is currently being explored. The purpose here is to discuss the mechanics of the crack arrest process for a mechanical arrester which is fabricated by loosely thread wrapping ductile steel wire rod around a segment of the pipe. The net effect of the wire rod arrester as the crack approaches is to substantially increase the axial in-plane strain in the pipe wall adjacent to the fracture path from the value it would have in the absence of the arrester. The result is that, in the presence of the arrester, the growth of a circumferential tensile fracture can become more favorable than continued growth of the axial tensile fracture, and a criterion for arrest of the axial fracture based on this result is proposed. Through an analysis of rapid crack propagation in a pressurized pipeline, the arrest criterion leads to an expression for the minimum ductility of the wire rod necessary for crack arrest. The required minimum ductility for the wire rod is estimated for system parameters corresponding to available full-scale test data, and the results compare favorably with the independently measured actual ductility of the arrester material.

Introduction

It is a common practice in the design and construction of large diameter pressurized pipelines to follow some sort of fracture control program in order to minimize the possibility of fracture initiation. Nonetheless, fractures can appear in such structures due to external sources, such as earth-moving equipment, or due to fabrication defects, for example. If occasional fracture initiation is regarded to be inevitable, then some precautions must be taken to localize the damage to the extent possible and to prevent the fracture from developing into a long, running crack. As operating pressures were increased to make transmission lines more efficient, it was first thought that long fractures would be precluded if construction materials were selected for which the brittle-ductile transition temperature was well below the minimum operating temperature of the pipeline. The main idea was that the gas decompression wave which would be generated upon fracture initiation would travel much faster than any possible ductile fracture, and therefore the crack driving pressure at the fracture initiation site would quickly be reduced to a level below that required to sustain crack growth. However, service failures of pressurized pipelines involving ductile shear fractures which have propagated long distances at very high rates have occurred.

With a view toward developing an understanding of this phenomenon, the American Iron and Steel Institute has sponsored a series of full-scale tests of large diameter pipe to determine the propagation and arrest characteristics of running ductile fractures. In these tests the pipe was instrumented with crack detectors, strain gages, and pressure transducers, and the electronically recorded data are summarized in [1, 2]. Test data on the same phenomenon were also reported in [3, 4]. Analytical models of ductile crack propagation in an initially pressurized line pipe have also been developed [5, 6, 7, 8]. These analytical investigations have not yet led to results which are adequately detailed to serve as basis for predicting material properties necessary for shear fracture arrest, although the analytical results have been coupled with empirical correlations between full-scale tests and Charpy impact tests to estimate minimum fracture toughness requirements for routine applications with some success. However, because of the difficulties which have been encountered in trying to establish material standards for arrest of shear fractures in line pipe for certain special applications, such as a line without backfill cover or a line carrying material which could undergo a phase change during sudden decompression, the possibility of introducing mechanical crack arresters has been considered [9]. One arrester configuration which performed very

Contributed by the Pressure Vessels and Piping Division for publication in the JOURNAL OF PRESSURE VESSEL TECHNOLOGY. Manuscript received at ASME Headquarters, August 11, 1978.

well in a recently conduct : full-scale test was fabricated by loosely thread wrapping ductile steel wire rod around a segment of the pipe. The purpose of this report is to present a discussion of the mechanics of the crack arrest process at such a wire-wrapped arrester with a view toward eventual design optimization of this configuration.

General Features of the Crack Growth Process

Before proposing a mechanical model for the arrester, it is useful to briefly review the main features of pipe deformation and gas pressure loading on the pipe walls during the crack propagation process in the absence of a mechanical arrester. These general features appear to be independent of absolute size scale, and all lengths are therefore expressed as multiples of the nominal radius of a pipe cross section, say a. At a position far from the fracture initiation site, the first motions which have been detected after initiation are due to elastic flexural waves in the pipe wall which travel at speeds between 600 and 1200 m/s. These transient flexural waves appear to arise from the fracture initiation process. The next disturbance to arrive at the observation point is due to the decompression wave in the gas which travels at a speed between 335 and 425 m/s, depending on the initial state and the mechanical properties of the gas. The decompression wave is generated as the gas, which was initially at equilibrium in the pressurized pipeline, begins to escape into the atmosphere through the opening fracture. Both the stress change due to the flexural waves in the pipe wall and the reduction in hoop stress associated with the gas decompression wave are well within the elastic range for typical materials and operating conditions. These aspects of the process are usually considered to be of minor importance and they are usually neglected in the development of analytical models of the process.

As the crack tip approaches to within about four or five radii of the observation position, very large in-plane extensional strains in the direction of crack propagation are typical. The origin of these in-plane axial strains becomes clear if the pipeline is viewed as a thin cylindrical shell, which is a legitimate idealization as long as the nominal cross-sectional radius is much larger than the wall thickness. In general, thin shells tend to deform predominately by bending, with minimal stretching of the middle surface. For a cylindrical shell, the only deformations satisfying strict inextensibility are those for which all generators of the cylinder remain straight during deformation. In the case of an axial fracture in a cylindrical shell, the generator ahead of the crack tip which forms the prospective fracture path is split by the crack into the two fracture surfaces. Behind the crack tip the shell walls flare outward and the crack faces separate. This deformation is clearly incompatible with each generator remaining straight, and some middle surface stretching must therefore occur during crack growth. Study of the shell strain-displacement relations suggests that the observed flaring of the walls is accompanied by stretching of the middle surface in the axial direction. Such stretching was observed to occur in the full-scale tests discussed in [1], where it was reported that large axial strains of up to 1 or 2 percent occurred in a band of total circumferential extent of about one radius.

The concentration of circumferential tensile stress ahead of the crack tip leads to large circumferential in-plane strains localized in a narrow band extending directly ahead of the tip. Thinning of the wall occurs within this band followed eventually by a partial-shear or full-shear fracture, depending on the toughness of the material.

The experimental data [1] suggest that the circumferential variation of internal pressure acting on the pipe wall is small, even near and behind the propagating crack tip, so that the pressure may be taken to be circumferentially uniform for most practical purposes. The pressure varies along the pipe in the decompression wave from the initial line pressure level at the decompression wavefront to a value between 30 percent and 100 percent of the line pressure level at the crack tip, depending on the crack-tip speed [3]. The pressure decays from its value at the tip to atmospheric pressure within about three to five radii behind the tip due to gas escape through the opening crack. It is widely believed at the present time that this residual gas pressure on the pipe walls behind the crack tip is the primary driving force for the crack propagation process. General plastic yielding of the pipewalls continues behind the crack tip until the pressure has decayed to a relatively small value and the outward acceleration of the walls is reversed due to material strength.

On the basis of the observations drawn from full-scale test data reported in [1, 2], an analytical model was recently developed [8] for ductile crack propagation in an initially pressurized long cylindrical shell. The analysis was directed toward the high toughness range of material behavior, for which extensive yielding occurs in the pipe walls, and the material was represented as being rigid-perfectly plastic. Further, to obtain a tractable model, the shell deformation was assumed to be steady as seen by an observer moving with the crack tip and kinematic assumptions were made so that the deformation was expressed in terms of a single function of the position along the shell axis which is determined in accordance with a variational statement of the equations of motion. Separation of material was represented by a Dugdale zone of localized yielding, in which a critical opening displacement is attained for fracture. With these approximations, the required pressure distribution decay length to drive the crack is estimated. In a separate study [10] concerned with the dynamics of gas escape through the opening crack, the pressure decay profile was estimated for the case of a widely opening crack. The estimate was in good agreement with the available experimental data. Other analytical models have been considered by Kanninen, et al. [5], Hahn, et al. [11], Emery, et al. [7] and Poynton, et al. [12]. A comparison of one-dimensional shell models was discussed in [13].

The Wire-Wrapped Mechanical Crack Arrester

The effectiveness as a crack arrester of wire rod loosely wrapped around the pipe was recently demonstrated in a full-scale experiment, the results of which are reported by Shoemaker, McCartney and Ives [9]. A steel pipe with a radius of 535 mm and a wall thickness of 19 mm was pressurized with air to a relative internal pressure of 11.5 MN/m^2, which simulated operating conditions at 323 MN/m^2 or 72 percent of the minimum yield strength. Beginning at a point about 10 m from the fracture initiation site, the pipe was loosely wrapped with two layers of hot-rolled steel wire rod having a diameter of 5.6 mm, a tensile yield strength of 578 MN/m^2, a nominal ultimate tensile strength of 959 MN/m^2, an elongation of 6.2 percent in a 25-cm gage length tensile specimen and a reduction of area of 46 percent at fracture. The specific fracture energy of the pipe material was estimated to be 5.52×10^5 J/m^2, which is the energy absorbed in 2/3 size CVN specimens averaged over the fracture area.

After the pipe was pressurized, a fracture was artificially induced in the pipe wall. The resulting crack tip propagating toward the rod-wrapped arrester quickly accelerated to a speed of about 300 m/s and it ran more or less steadily at this speed until it encountered the arrester. The crack tip passed under approximately the first 0.6 m of rod wrapping whereupon the crack propagation direction changed abruptly from axial to circumferential. The crack then extended as a *tensile shear fracture* for approximately 18 cm in the circumferential direction before the mode of fracture changed from tensile to tearing (out-of-plane shear). No further axial crack growth occurred and the crack was therefore successfully arrested. A few windings of the rod at the beginning of the wrapped section failed in tension. A noteworthy feature of the rod failure is that the windings appeared to undergo essentially *uniform* plastic strain over a circumferential distance of about 25 cm on either side of the fracture path and, in fact, many of the rods which fractured did so at points

other than directly over the crack path [9].

Model of the Arrest Process

Some general observations which are very helpful in guiding the development of an analytical model of the rod-wrapped arrester are the following:

1 It has already been noted that in the case of crack propagation in a linepipe without an arrester, the pipe wall undergoes large in-plane axial strains on the order of 1 percent along the fracture path as the crack tip approaches.

2 In the arrester experiment, strain gage records for points under the arrester along the fracture path suggest that much larger axial in-plane strains occur (in excess of 2 percent) as the crack begins to propagate under the arrester. That is, it appears that one effect of the arrester is to greatly increase the amount of *axial* in-plane strain of the pipe wall during fracture.

3 The fact that, upon the encounter with the arrester, the running fracture abruptly changes from an axial tensile fracture to a circumferential tensile fracture suggests that the combined arrester effects of increased axial in-plane strain and increased resistance to axial crack growth result in a situation in which it is easier for the existing loads to drive a circumferential crack than to drive an axial crack.

The viewpoint represented by these general observations is reinforced if the potential effect of a rod-wrapped arrester on in-plane axial strain is considered in light of the previous analysis of steady propagation without an arrester. An expression for the nominal axial strain near the crack tip along the fracture path is given in equation (34) of [8] as

$$\epsilon_\xi \simeq a\delta_t/R^2 \tag{1}$$

where a is the pipe cross-sectional radius, δ_t is the critical crack-tip opening displacement which must be achieved for fracture and R is the length of the localized plastic zone ahead of the crack tip. It is of particular interest to note how the *ductility* of a rod-wrapped arrester would influence ϵ_ξ. It seems to be reasonable to expect that the addition of a ductile circumferential wrapping would effectively increase the critical value of the crack-tip opening displacement, say δ_t^*, which would be required for continued axial crack growth, particularly if the wrapping would deform plastically over a significant portion of the circumference of the pipe as it did in the experiment. It should be emphasized that, according to this viewpoint, the quantity δ_t^* is the opening displacement which must be achieved to exhaust the ductility of *both* the pipe wall and the arrester material. Thus, the position of the crack tip coincides with the position of the last ruptured rod winding, which could be some distance behind the position of the tip of the crack in the pipe wall itself. Because the rod-wrapping has essentially no strength in the axial direction, its presence would not affect the value of crack opening displacement required for circumferential crack growth, say δ_c^*, which is just a property of the pipe wall material. From (1), it is clear that an increase in the crack opening displacement required for axial crack growth implies an increase in axial in-plane strain ϵ_ξ.

The influence of the arrester *strength* on ϵ_ξ can also be understood in terms of the analysis of [8]. A rough interpretation of the results presented there is that the total force due to the cohesive stress resultant acting along the length of the localized plastic zone, which represents the resistance to crack opening, must balance the total force exerted by the escaping gas on the pipe walls at and behind the crack tip, which represents the driving force for crack extension. One effect of the strength of the mechanical arrester is to increase the cohesive stress which can be transmitted across the plastic zone. For a given driving force, an increase in cohesive stress would be accompanied by a decrease in plastic zone extent R which, according to (1), implies an increase in axial strain ϵ_ξ.

Thus, it appears that the net effect of the ductility of the arrester, through δ_t^*, and the strength of the arrester, through R, is to substantially increase the axial strain from the value it would have in the absence of the arrester. The result that the main running axial crack arrests by first propagating as a tensile fracture in the circumferential direction therefore becomes quite plausible. In fact, if the viewpoint is taken that the arrester has been successful if a circumferential fracture is initiated, then an arrest criterion can be proposed. It is suggested that a running axial crack will be stopped at the arrester if, for specified geometrical and material parameters, the critical crack opening displacement for a circumferential tensile crack is reached before (i.e., at a lower driving pressure than) the critical opening displacement for continued axial crack growth through the arrester is reached, i.e., $\delta_c = \delta_c^*$ but $\delta_t < \delta_t^*$. It is hypothesized in [9] that the constraint of the deformation behind the crack tip in the pipe wall by the wire wrapping provides the means for crack arrest. This general idea is made more precise through the present analytical model, and quantitative estimates of the constraint required for arrest, measured through the mechanical properties of the wire rod, are made.

Equation of Motion for the Pipe Wall

The basic assumptions on which the present model is based are essentially the same as those discussed in detail in [8]. First, it is noted that the ratio of pipe wall thickness to mean pipe cross-sectional radius is generally small, and the theory of thin shells [14] is assumed to be applicable. The available data [1] implies that, after a crack tip has advanced a distance of about four diameters from the initiator, the fracture process is insensitive to the crack length and the growth process is steady as seen by an observer moving with the crack tip. Thus, it is assumed that the crack is semi-infinite in length, that it moves at constant speed along a generator of the cylindrical pipe, and that the deformation field is time-independent as seen by an observer moving with the crack tip. Clearly, the crack arrest process of ultimate interest is not a steady-state process. If mechanical conditions which are necessary to sustain a running steady-state fracture can be established, however, then it may be reasonable to infer that if these conditions are not met then the crack will arrest.

To render the problem tractable, it is assumed that the entire deformation field of the shell is determined by a single function of the axial coordinate. With the experimental results of [1] as guidance, a deformation field is hypothesized which leads to neither in-plane circumferential strains nor in-plane shear strain of the pipe wall. Axial in-plane strain of the pipe wall appears to be important, as already noted, and the possibility of such extensional strain is included. It is noteworthy that, for most shell problems, the main effects introduced through a large deflection formulation are associated with the membrane deformations of the shell. In the present problem membrane effects are already included through the axial in-plane strain. Thus, the additional complexity which would be introduced through a large deflection formulation cannot be justified in a first analysis of the arrester problem, and a small deflection formulation is employed.

The Deformation Field. Spatial coordinates on the shell surface are defined in Fig. 1. The mean radius of the undeformed shell is a, the shell thickness is h, the circumferential coordinate is θ, and the axial coordinate is ξ, the origin $\xi = 0$ being fixed at the moving crack tip. If x is a spatially fixed axial coordinate and V is the speed of the crack tip, then $\xi = Vt - x$. Because of the assumption of a steady-state deformation, all field variables depend on x and t only through ξ. The crack faces coincide with the lines $0 < \xi < \infty$, $\theta = 0, 2\pi$ on the shell.

The axial, circumferential and normal components of the displacement vector of a point initially at (ξ, θ) on the shell midsurface are denoted by u, v, w, respectively. The assumed displace-

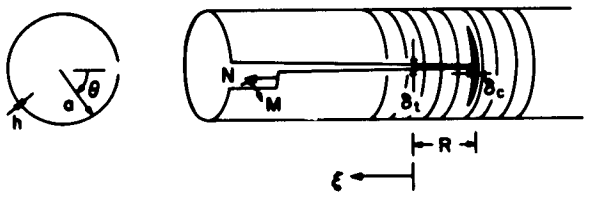

Fig. 1 Geometry of crack propagation and bifurcation in a pressurized pipeline

ment field is expressed in terms of a single unknown function of axial coordinate, say $\phi(\xi)$, by

$$w = \phi(\xi)\left(\frac{\pi}{2} - \theta\right) \tag{2}$$

$$v = \frac{1}{2}\phi(\xi)\left(\frac{\pi}{2} - \theta\right)^2 \tag{3}$$

$$u = \frac{1}{6}a\phi'(\xi)\left(\frac{\pi}{2} - \theta\right)^3 \tag{4}$$

for $0 < \theta < \pi/2$. The pipe wall is assumed to remain undeformed for $\pi/2 < \theta < \pi$, and the entire deformation field is assumed once and for all to be symmetric with respect to reflection in the plane $\theta = 0$. The displacement field (2, 3, 4) was constructed by assuming that each initially circular cross section deforms through outward flaring of the walls adjacent to the crack line over a circumferential distance of $a\pi$, and then by requiring that the circumferential and shear strains of the middle surface vanish. Clearly, continuity of displacement along the line $\theta = \pi/2$ is satisfied. The nonzero strains derived from the displacement field (2), (3), (4) are

$$\epsilon_\xi = \frac{\partial u}{\partial \xi} = \frac{1}{6}a\phi''(\xi)\left(\frac{\pi}{2} - \theta\right)^3 \tag{5}$$

$$\kappa_\xi = -\frac{\partial^2 w}{\partial \xi^2} = -\phi''(\xi)\left(\frac{\pi}{2} - \theta\right) \tag{6}$$

$$\kappa_\theta = -\frac{1}{a^2}\frac{\partial^2 w}{\partial \theta^2} + \frac{1}{a^2}\frac{\partial v}{\partial \theta} = -\frac{1}{a^2}\phi(\xi)\left(\frac{\pi}{2} - \theta\right) \tag{7}$$

$$\kappa_{\xi\theta} = -\frac{1}{a}\frac{\partial^2 w}{\partial \xi \partial \theta} + \frac{1}{a}\frac{\partial v}{\partial \xi} = \frac{1}{a}\phi'(\xi)\left[1 + \frac{1}{2}\left(\frac{\pi}{2} - \theta\right)^2\right] \tag{8}$$

where ϵ_ξ is axial strain, κ_ξ and κ_θ are changes in axial and circumferential curvature of the middle surface, and $\kappa_{\xi\theta}$ is the change in torsion of the middle surface.

The restriction of the deformation to the range $0 < \theta < \pi/2$ seems to be the simplest way of introducing a circumferential cohesive zone because this zone may then be taken to extend over the same angular range as the deformation itself and, furthermore, continuity of displacement is automatically satisfied over the complementary range of θ. Although it could be assumed from the outset that the deformation extends over a range of θ less than $\pi/2$, the choice of $\pi/2$ is most consistent with observation [1, 2]. For example, the waviness in the pipe wall known as "scalloping" which appears on either side of the fracture path as a result of axial buckling after inhomogeneous axial straining extends for a total circumferential distance of about $a\pi$ in a typical full-scale test. If the pipe wall material is assumed to be perfectly plastic (as will be done subsequently) then an angular range greater than $\pi/2$ for the deformation may be ruled out by assuming that the net axial force on a cross section is zero and noting that the axial stress in the nondeforming sector must be at or below the tensile yield stress.

The deformation field (2), (3), (4) results in zero circumferential strain, while the measurements indicate the occurrence of significant circumferential strains near the crack line ahead of the crack tip. This is taken into account in the model by including a one-dimensional plastic zone of the Dugdale type [15] ahead of the advancing crack tip. In effect, this concentrates all of the circumferential strain in this one-dimensional plastic zone which occupies the interval $\theta = 0$, $R < \xi < 0$ as shown in Fig. 1, where the plastic zone size R is to be determined as part of the solution. The pipe wall remains undeformed for $0 < \theta < 2\pi$, $\xi < -R$. Within the plastic zone, relative motion of the crack faces is resisted by a cohesive force per unit length along the middle surface, say $T(\xi)$. In the presence of the rod-wrapped arrester, the plastic zone is viewed as the region over which both the pipe wall and the rods are undergoing large circumferential strains, and the axial crack tip is defined to be the point at which fracture of both the pipe wall and the rod material has been completed. In a sense, the arrester is viewed as an integral part of the shell structure and its presence is accounted for through its effect on the force transmitted across the cohesive zone and on the critical value of crack opening displacement which must be achieved to complete the fracture process. The amount of crack opening $\delta(\xi)$ is given generally by

$$\delta(\xi) = -2v(\xi, 0) = \pi^2\phi(\xi)/4 \tag{9}$$

and the axial crack-tip opening displacement is

$$\delta_t \equiv \delta(0) = \pi^2\phi(0)/4. \tag{10}$$

For steady crack propagation in a pipeline without an arrester, the displacement is continuous everywhere except on the crack line. On the other hand, it has already been noted that a running axial fracture tends to form tensile shear fractures in the circumferential direction upon encountering a rod-wrapped arrester. To include this possibility in the model analysis, it is assumed that a one-dimensional zone of localized tensile plastic yielding extends from the tip of the axial plastic zone in the circumferential direction over a distance of $a\pi/2$ on either side of the main fracture, as shown in Fig. 1. The deformation due to localization of axial extensional strain in these zones is taken into account by permitting a discontinuity in axial displacement u across the zones. In view of the assumed displacement field (2), (3), (4) the opening displacement along this cohesive zone may be completely specified by the opening displacement at $\theta = 0$, say δ_c, which is given by

$$\delta_c \equiv u(-R, 0) = a\phi'(-R)\pi^3/48\ . \tag{11}$$

Of course, these circumferential cohesive zones are also plastic zones of the Dugdale type, and relative opening across the circumferential cohesive zones is resisted by a tensile force per unit length along the middle surface, this force depending on the flow properties of the pipe wall material. The rod-wrapped arrester has no influence on the resistance of the structure to circumferential crack growth, and therefore the arrester has no influence on the cohesive stress transmitted across the circumferential cohesive zones.

Distribution of Applied Pressure. The applied loading in this problem is the internal pressure. According to available data, it is reasonable to assume that the pressure distribution acting on the pipe wall is a function of axial coordinate, say $p(\xi)$, but is independent of the angular coordinate θ. Also, according to the data, the pressure may be taken to be uniform within the cohesive zone interval $0 > \xi > -R$, and the magnitude there is equal to the velocity dependent crack tip pressure proposed by Maxey, et al. [3], i.e.,

$$\frac{p_o(V)}{P_L} = \left[\frac{2}{\nu + 1} + \frac{(\nu - 1)V}{(\nu + 1)c_L}\right]^{\frac{2\nu}{\nu-1}} \tag{12}$$

where p_L and c_L are line pressure and sonic speed of the gas at $\xi \to -\infty$, and ν is the ratio of specific heat at constant pressure to specific heat at constant volume for the gas; for example, $\nu = 7/5$ for air. Behind the moving crack tip, the pressure is assumed to decay continuously from p_j at the tip to zero at some distance, say λ, behind the crack tip. Thus, to complete the definition,

$$p(\xi) = \begin{cases} p_o & -R < \xi < 0 \\ p(\xi) & 0 < \xi < \lambda \\ 0 & \lambda < \xi < \infty \end{cases} \tag{13}$$

The results of [10] suggest that the pressure decay profile, p/p_o versus ξ/a, is insensitive to variations in p_0 for widely opening cracks and that the decay length is approximately $4a$.

Equation of Motion for Rigid-Perfectly Plastic Material. The fundamental physical principle governing the deformation of the shell is taken to be the principle of virtual work. For any deformable body the principle can be stated in terms of any equilibrium distribution of internal stresses or generalized stresses which balance the applied loads (including, by d'Alembert's principle, the inertial forces) and any unrelated distribution of compatible strains and associated displacements. The application of the virtual work principle to a problem of the type being considered here was discussed in detail in [8]. Thus, after a brief review of the main assumptions, only the equation of motion resulting from application of the principle is included here.

Preliminary analyses of the problem indicated that for deformations of the type (2), (3), (4) the energy dissipation through internal plastic work associated with the axial stretching and circumferential bending modes is much greater than that associated with the axial bending and the torsional modes, and the latter contributions are therefore neglected in writing the virtual work equation. Furthermore, the inertial effects in the normal and circumferential directions appear to be much larger than in the axial direction, and the axial inertial force is also neglected in the virtual work equation.

The only generalized stresses which appear in the virtual work equation are N, the axial force per unit length along the middle surface of the shell, and M, the circumferential bending moment per unit length, as shown in Fig. 1. The plastic yield surface for the shell, represented in terms of N and M, is shown in Fig. 2. The dashed curve is the exact yield surface which is determined in [16] according to the bounding theorems of plastic limit analysis and a Tresca yield condition. As in [8], the analysis is greatly facilitated if the exact yield surface is approximated by the solid line in Fig. 2. The axes are normalized with respect to N_o and M_o, the yield resultants in pure extension and pure bending, respectively, which are given by

$$N_o = \sigma_o h, \; M_o = \sigma_o h^2/4 \tag{14}$$

where σ_0 is the tensile flow stress of the material. Finally, consistent with the idealized rigid-plastic description of material behavior and with the kinematic assumptions adopted here, M and N can be considered to be circumferentially uniform in any deforming region and independent of θ. Following the analysis of [8], the principle of virtual work yields the field equation governing the deformation in the form of an ordinary differential equation, viz.,

$$\frac{\pi^2}{48} a^2 N''(\xi) = ap(\xi) - T(\xi) - \frac{1}{a} M(\xi) - \rho V^2 a \left(\frac{\pi^3}{80} + \frac{\pi}{3} \right) \phi''(\xi) \tag{15}$$

where ρ is the mass density per unit area of the middle surface. The differential equation is augmented by the boundary conditions

$$\phi(-R) = 0, \; \phi'(-R) = 48\delta_c/a\pi^3 \tag{16}$$

$$N(-R) = 0.75\, N_o, \; N'(-R) = 0 \tag{17}$$

The first condition of (16) ensures continuity of normal displacement across $\xi = -R$, and the second condition of (16) is a restatement of (11) in which the discontinuity in axial displacement is expressed in terms of the circumferential cohesive zone opening displacement. If the circumferential cohesive zone exists, the stress transmitted across this zone must be the tensile yield stress, as in the first condition of (17). Because there are no concentrated forces at $\xi = -R$, N must vary smoothly there and $N'(-R) = 0$ to avoid violation of the yield condition.

The solution is made determinate by requiring the strain rate vector to be normal to the yield surface in plastically deforming regions. The axial stretching rate $\dot{\epsilon}_\xi$ is proportional to ϕ''' and the circumferential curvature rate $\dot{\kappa}_\theta$ is proportional to $-\phi'$. Thus, for a stress state on $N = 0.75\, N_0$, on $M = M_0$ or on the intersection point of these two lines,

$$N = 0.75\, N_o, \; |M| < M_o \text{ and } \phi' = 0, \tag{18}$$

$$|N| < 0.75\, N_o, \; M = M_o \text{ and } \phi''' = 0, \tag{19}$$

$$N = 0.75\, N_o, \; M = M_o \text{ and } 0 < -\phi'''/\phi' < \infty, \tag{20}$$

respectively, with similar relationships holding on other sides and corners of the yield locus. In an interval in which (18) is satisfied, ϕ is constant and no deformation occurs. In an interval in which (19) is satisfied, ϕ'' is constant. Thus, the axial strain and axial curvature are constant but the walls may flare outward because the circumferential curvature rate is not zero. In an interval in which (20) is satisfied, $N'' = 0$ and the equation of motion (15) implies that the shell wall will deform *inward* if $T + M/a$ is greater than ap, as it is near the crack tip. Such behavior is unrealistic and it is unlikely that the solution will correspond to the conditions in (20) over any intervals, although it may do so for discrete values of ξ. Because these are the only types of plastically deforming regions which may exist, a possible description of the general features of the deformation field emerges. The plastically deforming section of the pipe $\xi > -R$ must be divided into intervals in each of which $|N| < 0.75\, N_o$ and $\phi''(\xi)$ is constant. The value of ϕ'' is different in adjacent intervals so that ϕ'' is discontinuous across the interval end point.

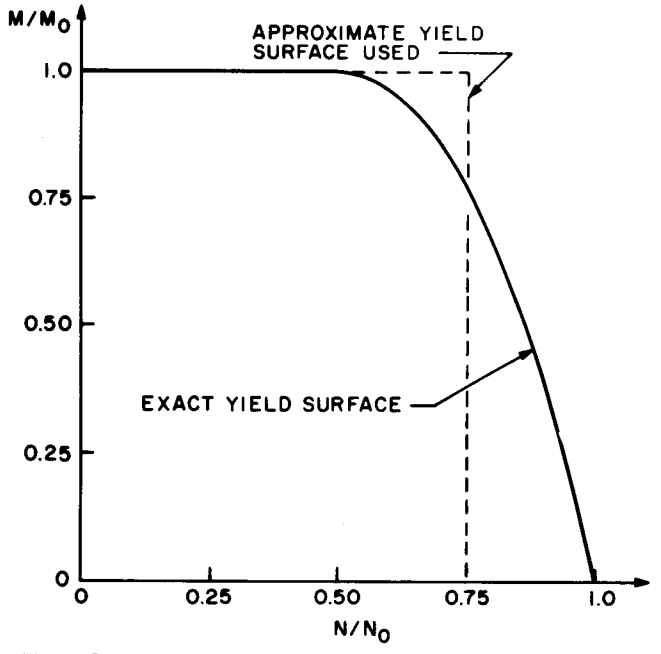

Fig. 2 One quadrant of the exact and approximate yield surfaces for the generalized stresses N and M shown in Fig. 1

Discontinuous ϕ'' at a point implies an unbounded ϕ''' there so that, according to (20), the stress state at any end point of these intervals must coincide with a corner of the yield locus. A solution having precisely these features was found in the analysis of crack propagation in a pressurized pipeline without an arrester [8].

Solution

If the specified values of the material, geometrical and loading parameters are such that a solution exists, then a solution having the general features outlined in the foregoing may be constructed by following the procedure in [8]. A typical crack opening profile $\delta(\xi)$ for the problem at hand is shown in Fig. 3. Recall the relation $\delta(\xi) = \pi^2\phi(\xi)/4$ from (9). For $\xi < -R$, $\delta(\xi) = 0$ and the constant value of ϕ'' is zero. At $\xi = -R$, the value of ϕ'' changes from zero to some other constant value, say $\phi_o'' > 0$, and this value is maintained in the interval $-R < \xi < \lambda_1$ where $\lambda_1 > 0$. The shell walls are thus moving outward and accelerating in this interval. At $\xi = \lambda_1$, ϕ' is continuous but the value of ϕ'' jumps from ϕ_o'' to some other constant value, say $\phi_1'' < 0$, and this value is maintained in the interval $\lambda_1 < \xi < \lambda_2$. In this interval, the shell walls continue to move outward but with negative acceleration. At $\xi = \lambda_2$, ϕ' is continuous and equal to zero so that the shell is at rest and remains at rest for $\xi > \lambda_2$. The value of ϕ'' changes from ϕ_1'' to zero at $\xi = \lambda_2$. The values of R, λ_1 and λ_2 are determined as part of the solution from continuity conditions on traction and displacement. In summary, the opening profile in Fig. 3 consists of two parabolas, one with positive curvature and one with negative curvature. The slope is continuous everywhere except at $\xi = -R$, where the discontinuity arises from the circumferential cohesive zone; cf. (16). If $\phi''(-R + 0) = \phi_o''$ and $\phi'(-R + 0) = \phi_o'$ then the functional form of the opening profile in the interval $-R < \xi < \lambda_1$ is

$$4\delta(\xi)/\pi^2 = \phi(\xi) = \frac{1}{2}\phi_o''\xi^2 + (R\phi_o'' + \phi_o')\xi + \left(\frac{1}{2}R\phi_o'' + \phi_o'\right)R \qquad (21)$$

The constants ϕ_o' and ϕ_o'' may be expressed in terms of physical parameters of the system through (10) and (11) as

$$\phi_o' = 48\delta_c/a\pi^3\,,\quad \phi_o'' = 8(\delta_t - 12R\delta_c/a\pi)/\pi^2R^2 \qquad (22)$$

From (5), it can be seen that the extensional strain ϵ_ξ along the crack line $\theta = 0^+$ in the interval $-R < \xi < \lambda_1$ is a constant, say ϵ_o,

$$\epsilon_\xi = \epsilon_o = a\pi^3\phi_o''/48 \qquad (23)$$

Comparison of (22) and (23) yields the relationship

$$\frac{6}{\pi}\left(\frac{R}{a}\right)^2 a\epsilon_o + \frac{12}{\pi}\frac{R}{a}\delta_c = \delta_t \qquad (24)$$

The result (24) has been derived mainly from the kinematics of the problem and from material characteristics, without solving the equation of motion (15). Nonetheless, it seems that (24) is of potential use in the design of a wire-wrapped crack arrester because the parameters appearing in (24) can be estimated without difficulty. A typical calculation is made in the following section. It should be recalled that (24) was derived under the assumption of steady crack propagation, i.e., if the system parameters are such that (24) holds then steady crack propagation occurs. From a practical point of view, an alternate viewpoint is taken, i.e., if the system parameters are such that the actual value of the left side of (24) is less than the opening displacement which can be accommodated by the arrester δ_t^*, then the arrester will be adequate to stop a running fracture.

The equation of motion (15) may be solved by following the procedure outlined in [8], where the solution procedure is described in detail for arbitrary pressure but without inertial effects included. However, inertial effects may be easily included in the solution procedure by means of an iteration scheme. The problem is first solved for the assumed pressure distribution and with the inertial term set equal to zero, resulting in first estimates for the values of the length parameters R, λ, λ_1 and λ_2. Then, for specified values of δ_c and δ_t, a deformation field corresponding to these length parameters may be determined. The applied pressure is then reduced by an amount equal to the inertial forces arising from this deformation field and the problem is solved once again for this modified pressure which leads, in turn, to new estimates of the length parameters, the deformation field, the inertial forces, the effective pressure, and so on. The iteration is continued until the successive estimates converge to a solution for which all conditions are satisfied to within some pre-set accuracy. Some numerical results are discussed in the next section.

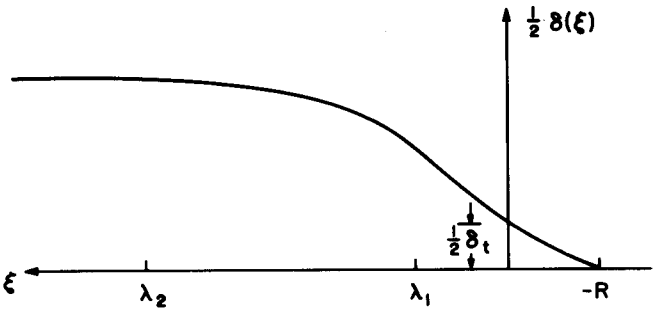

Fig. 3 Schematic representation of the crack-opening profile, consisting of two parabolic segments in $-R < \xi < \lambda_1$ and $\lambda_1 < \xi < \lambda_2$

Results and Discussion

The result (24) is now considered in light of the data reported by Shoemaker, McCartney and Ives [9] from the full scale test which was discussed in the Introduction. First, estimates of the actual values of the parameters R/a, ϵ_o and δ_c will be substituted into the left side of (24) to obtain a reasonable estimate of the minimum crack-tip opening displacement required for crack arrest. This estimate can then be compared to the attainable opening displacement corresponding to the independently measured ductility of the wire rod used to form the arrester.

According to theoretical analysis [8], the plastic zone size R for steady-state propagation without an arrester is typically equal to about one pipe radius a, and it is virtually always less than $2a$. For steady-state crack propagation with an arrester R/a is typically less than one. For numerical values of the parameters being considered here, solution of the equation of motion (15) led to the estimate R/a $\simeq$ 0.2. Thus, a reasonable range of values for R/a seems to be from about 0.2 to 1, and the upper limit $R/a = 1$ is chosen for the calculation here. An estimate of the pipewall ductility δ_c^* is obtained from 2/3 CVN test data assuming that the energy absorbed per unit area in the Charpy specimen is equal to the product of the yield stress of the material times δ_c^*. Thus, $\delta_c^* = (5.52 \times 10^5\ \mathrm{J/m^2}) \div (5.78 \times 10^8\ \mathrm{N/m^2}) \simeq 0.1$ cm. It should be noted that this estimate ignores the effects of the plane strain type of constraint which is operative in the crack-tip region in the center portion of the Charpy specimen. Inclusion of the constraint effect could lower the estimate by perhaps 50 percent. A reasonable range of values for δ_c^* seems to be from about 0.05 cm to 0.1 cm, and the upper limit $\delta_c^* = 0.1$ cm is chosen for the calculation here. The actual value of the parameter ϵ_o, say ϵ_o^*, is a measure of the uniform extensional strain which can be accommodated by the pipe wall material before the deformation localizes and the circumferential

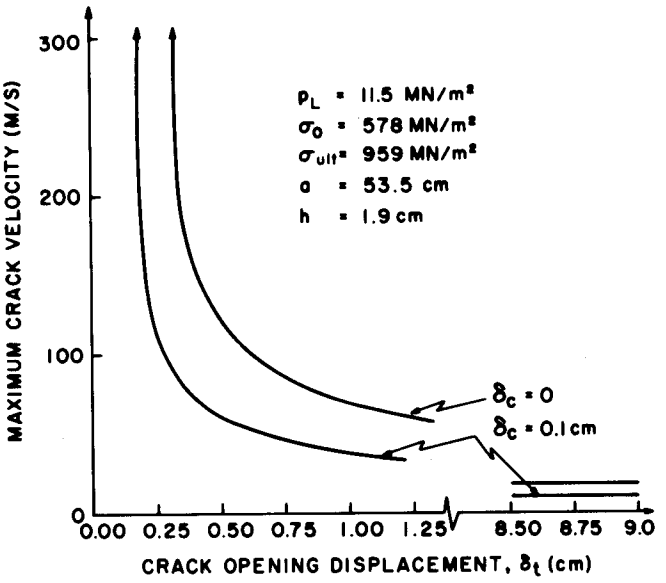

Fig. 4 Computed maximum attainable steady-state crack-tip velocity versus crack-opening displacement δ_t for the data reported in [9]

cohesive zone is formed. The study of strain localization in biaxially stretched thin sheets has begun only very recently, and a firm estimate of ϵ_o^* cannot yet be given. Uniform extensional strains of up to 0.02 have been observed in the crack-tip region in the full-scale tests so that this value serves as a reasonable lower bound on the range of values of ϵ_o^*. An upper bound may be determined by noting that the extensional strain prior to fracture in the region of deformation localization is given approximately by δ_c^*/h which, for $\delta_c^* = 0.1$ cm and $h = 1.9$ cm, is approximately 0.05. Thus, a reasonable range of values for ϵ_o^* seems to be from 0.02 to 0.05 and, because the upper bound is an extreme estimate, the value of $\epsilon_o^* = 0.03$ is chosen for the present calculation. It might be noted that this estimate is not inconsistent with theoretical estimates for low-hardening materials obtained by Stören and Rice [17]. With these values of the parameters R/a, ϵ_o^* and δ_c^*, and with radius $a = 53.5$ cm, an estimate of the required crack tip opening displacement is obtained as $(\delta_t)_{req} = 3.5$ cm. An examination of the wire rods after the crack was arrested in the test [9] reveals that the plastic strain in the wires was quite uniform over a large circumferential distance on either side of the crack line. It thus seems reasonable to assume that the strain in the wire rod resulting in the opening δ_t is uniform over the full range $-\pi/2 < \theta < \pi/2$, so that this strain is $(\delta_t)_{req}/\pi a = 0.02$. Thus, the ductility requirement on the arrester material is that it must undergo 2 percent *uniform* elongation prior to failure. It is reported in [9] that 25.4-cm tension specimens of the wire rod material were tested in the laboratory, with a uniform elongation of 6.2 percent prior to fracture. Thus, the actual ductility of the arrester material exceeds the estimate of required ductility and the result is consistent with the fact that the arrester was indeed successful in stopping the running fracture. The more conservative estimate $(\delta_t)_{req} = 9.8$ cm, which is obtained by assuming $R/a = 1.5$ and $\epsilon_o^* = 0.04$, leads to a uniform elongation requirement of 5 percent strain for the rod material (all other quantities being unchanged from the previous case). It is noteworthy that this estimate is still less than the measured ductility of the arrester material.

A particular result obtained through numerical solution of the equation of motion (15) is shown in Fig. 4. All material, geomettrical, and loading parameters except δ_t and V were selected to correspond to the data which were reported in [9] and which are summarized in the above section in which the process is described. The value of the crack-tip opening displacement or ductility δ_t was fixed, and the equation of motion was solved for some small value of speed V. If a solution existed, the value of V was increased and the equation of motion was again solved. This procedure was continued until a value of speed V was reached for which a steady-state solution did not exist. This process was repeated for many values of δ_t and the graph in Fig. 4 was generated. The curve represents the maximum possible velocity at which a crack can propagate steadily versus the crack-tip opening displacement δ_t. Steady-state solutions do not exist for points above the curve. Which of the steady-state solutions corresponding to points below the curve actually represents a particular process depends on the gas dynamics of the problem, as discussed in [8]. Before the propagating crack encounters the arrester, axial crack growth is more favorable than circumferential crack growth, and the fracture proceeds without formation of a circumferential cohesive zone. The formation of a circumferential cohesive zone without an arrester could be simulated by taking $\delta_c^* = \delta_t^*$ but, except for extremely small values of δ_t^*, steady-state solutions satisfying this condition could not be found. For the present example, the crack grows with $\delta_c = 0$ and $\delta_t = 0.1$ cm prior to its encounter with the arrester and, as can be seen from Fig. 4, very large crack speeds which approach the sonic speed of the gas are possible. The effect of the arrester is to increase δ_t^* to a value much larger than δ_c^* which significantly reduces the maximum possible speed for crack propagation. If the arrester is successful, of course, then circumferential crack growth becomes more favorable than axial growth and the velocity of axial crack propagation is reduced to zero. It should be emphasized that the proposed arrest criterion embodied in equation (24) is quite independent of the steady growth solutions of the equation of motion, (15), which are shown in Fig. 4, and, indeed, no attempt to incorporate arrest criteria into this figure has been made. Rather, the figure illustrates general features of the present model; for example, that for low δ_t values, the maximum attainable crack velocity can reach very large values, approaching the sonic speed of the gas, while this maximum attainable velocity decreases quite sharply over a narrow range of δ_t values.

Finally, several points concerning the wire-wrapped mechanical crack arrester are noted:

1 The net effect of the wire-wrapped arrester is to increase resistance of the structure to axial crack propagation (through an increase in the critical value δ_t^*) and to increase the driving force for circumferential tensile crack growth (through a reduction in R and a corresponding increase in ϵ_ξ). These directional properties may be enhanced through the fabrication induced anisotropy of the pipe wall itself. For example, processes leading to material microstructures with particularly low resistance to crack growth in the circumferential direction would be favorable.

2 Rate-sensitivity of the material was not taken into account in this study, although an adjustment in the magnitudes of yield stress and ultimate stress could easily be made to account for rate effects. It was noted in [9] that the behavior of the wire rod in the full-scale test was virtually identical to that observed in quasi-static laboratory tests, and it is unlikely that rate effects play a dominant role in the process.

3 For the wire-wrapped arrester to be successful, it is absolutely essential that the wire rod experiences extensive strain over a significant portion of the circumference on either side of the crack line. Only in this way can the total elongation, which is equivalent to δ_t^*, be increased to a sufficiently large value so that circumferential crack growth is initiated. It should be noted that the tendency for uniformity of straining increases with an increase in strain hardening of the rod material.

4 The actual strength of the wire rod does not directly enter the main result (24), although it does enter the equation of motion (15) through its contribution to $T(\xi)$. Even though the rod material exhibits significant strain hardening, it was modeled for this purpose as a rigid-perfectly plastic material with tensile flow

stress equal to the average of the measured tensile yield stress and ultimate tensile stress. As argued previously, the plastic zone size R is inversely proportional to the strength of the wire rod, all other things being equal, so that the strength does enter indirectly into (24). On this basis, it might be argued that a value of R/a less than one would be more suitable if the net arrester strength in the circumferential direction is comparable to the shell wall strength. Because of the transient nature of the arrest process and other uncertainties involved, perhaps the more conservative estimate is suitable for the time being.

5 Because of the nature of the model, the length of the wrapped section did not enter the formulation. However, it would seem that if an arrester is going to be effective, it will not permit any sort of steady crack propagation and arrest should occur within a short distance. Perhaps a length equal to $2a$ or $3a$ would suffice.

Acknowledgment

We are grateful to A. K. Shoemaker of the U. S. Steel Research Laboratories and J. E. Hood of The Steel Company of Canada for helpful discussion of this work.

This work was supported in part by the Committee of Large Diameter Line Pipe Producers of the American Iron and Steel Institute, and in part by the National Science Foundation through Grant No. ENG 77-15564 to Brown University.

References

1 Ives, K. D., Shoemaker, A. K., and McCartney, R. F., "Pipe Deformation During a Running Shear Fracture in Line Pipe," ASME *Journal of Engineering Materials and Technology*, Vol. 96, 1974, pp. 309–317.

2 Shoemaker, A. K., and McCartney, R. F., "Displacement Considerations for a Ductile Propagating Fracture in Line Pipe," ibid., pp. 318–322.

3 Maxey, W. A., Kiefner, J. F., Eiber, R. J., and Duffy, A. R., "Experimental Investigation of Ductile Fractures in Piping," *Proceedings of the 12th World Gas Conference*, International Gas Union, Nice, 1973.

4 Maxey, W. A., Kiefner, J. F., Eiber, R. J., and Duffy, A. R., "Ductile Fracture Initiation, Propagation, and Arrest in Cylindrical Vessels," *Fracture Toughness*, ASTM-STP 518, 1972, pp. 70–81.

5 Kanninen, M. F., Sampath, S. G., and Popelar, C., "Steady-State Crack Propagation in Pressurized Pipelines Without Backfill," ASME JOURNAL OF PRESSURE VESSEL TECHNOLOGY, Vol. 98, 1976, pp. 56–65.

6 Poynton, W. A., and Fearnehough, G. D., "An Analysis of Ductile Fracture Propagation in Gas Pipelines," *Dynamic Crack Propagation*, ed., G. C. Sih, Noordhoff, 1974, pp. 183–196.

7 Emery, A. F., Love, W. J., and Kobayashi, A. S., "Dynamic Finite Difference Analysis of an Axially Cracked Pressurized Pipe Undergoing Large Deformations," *Fast Fracture and Crack Arrest*, ASTM-STP 627, 1977, pp. 143–158.

8 Freund, L. B., Parks, D. M., and Rice, J. R., "Running Ductile Fracture in a Pressurized Line Pipe," *Mechanics of Crack Growth*, ASTM-STP 590, 1976, pp. 243–262.

9 Shoemaker, A. K., McCartney, R. F., and Ives, K. D., "Mechanical Crack-Arrester Concepts for Line-Pipe Applications," presented at the Conference on Materials Engineering in the Arctic, St. Jovite, Quebec, 1976.

10 Parks, D. M., and Freund, L. B., "On the Gasdynamics of Running Ductile Fracture in a Pressurized Line Pipe," ASME JOURNAL OF PRESSURE VESSEL TECHNOLOGY, Vol. 100, 1978, pp. 13–17.

11 Hahn, G. T., Sarrate, M., Kanninen, M. F., and Rosenfield, A. R., "A Model for Unstable Shear Crack Propagation in Pipes Containing Gas Pressure," *International Journal of Fracture*, Vol. 9, 1973, pp. 209–222.

12 Poynton, W. A., Shannon, R. W. E., and Fearnehough, G. D., "The Design and Application of Shear Fracture Propagation Studies," ASME *Journal of Engineering Materials and Technology*, Vol. 96, 1974, pp. 323–329.

13 Freund, L. B., and Parks, D. M., discussion of reference [5], ASME JOURNAL OF PRESSURE VESSEL TECHNOLOGY, Vol. 98, 1976, pp. 323–324.

14 Novozhilov, V. V., *Thin Shell Theory*, transl., P. G. Lowe, Noordhoff, Groningen, 1964.

15 Dugdale, D. S., "Yielding of Steel Sheets Containing Slits," *Journal of the Mechanics and Physics of Solids*, Vol. 8, 1960, pp. 100–104.

16 Hodge, P. G., Jr., *Plastic Analysis of Structures*, McGraw-Hill, New York, 1959.

17 Stören, S., and Rice, J. R., "Localized Necking in Thin Sheets," *Journal of the Mechanics and Physics of Solids*, Vol. 23, 1975, pp. 421–441.